A New Relaxation Effect with Polymer Depletion Layers

ARTICLE *in* LANGMUIR · DECEMBER 1996

Impact Factor: 4.46 · DOI: 10.1021/la9604893

5 AUTHORS, INCLUDING:

Dirk Walther
Max Planck Institute of Molecular Plant Physi…

91 PUBLICATIONS **3,662** CITATIONS

SEE PROFILE

A New Relaxation Effect with Polymer Depletion Layers

E. Donath,[†] D. Walther,[‡] A. Krabi,[§] G. C. Allan,[||] and B. Vincent*,[||]

Department of Internal Medicine, University of Rostock, Rostock D-18051, Germany, Department of Biocomputing, EMBL Heidelberg, Heidelberg, Germany, MPI for Colloid and Interface Research, Berlin, Germany, and School of Chemistry, University of Bristol, Cantock's Close, Bristol BS8 1TS, U.K.

Received May 20, 1996. In Final Form: September 9, 1996[⊗]

Dynamic light scattering measurements of the apparent radius of small lipid liposomes in the presence of depletion layer forming dextran with a molecular weight of 110 and 500 kD demonstrated a relative decrease of the depletion effect with decreasing particle radius and increasing molecular weight. To explain this unexpected behavior the static view of the depletion effect near a resting wall has been modified by introducing the concept of a depletion layer formation time. If the latter is comparable to the time the particle requires to diffuse over a distance equal to the depletion layer thickness, the depletion effect should be reduced. This new effect was termed depletion layer relaxation. An estimate of the depletion layer formation time was derived by means of Brownian dynamics simulations of free dextran without and with hydrodynamic interaction. The power law of the autocorrelation time as a function of the polymer radius was calculated. At high polymer coverage, where ensemble averaging is meaningful, the depletion layer formation time is given by the autocorrelation time of the polymer radius. At low coverage the depletion layer formation time is larger by 1 order of magnitude. An analytical formula is provided in a linear approximation.

Introduction

Polymer depletion layers and polymer adsorption layers are of both practical and theoretical interest.[1] While polymer adsorption layers at particle surfaces have been extensively studied both experimentally and theoretically by a variety of methods, appropriate techniques for the investigation of polymer depletion layers started to develop only recently.[2−4] One of the major directions for characterizing depletion layers has been to study the equilibrium thermodynamic properties of colloidal dispersions, in particular the colloidal stability as a function of various parameters.[5−9]

In a recent series of papers we showed that polymer depletion zones can also be characterized in terms of their rheological coefficients.[10,11] The basic assumption is that, due to the reduced polymer segment density in the depletion zone, the local viscosity is smaller than that in the bulk polymer solution. Electrokinetic measurements proved to be especially appropriate. The electrophoretic mobility depends only on the viscosity in the region of the diffuse part of the double layer. From electrophoretic experiments we were able to derive the extension of depletion layers for a variety of systems.[12,13] So far, measurements have been restricted to charged particles in aqueous systems.

Quite recently, the hydrodynamic resistance of particles with depletion layers was also calculated.[14] It was *a priori* clear that, given the small thickness of depletion layers (being on the order of the radius of gyration of the polymer), only in the case of particles not too large compared to the polymer radius of gyration is the effect of depletion on the hydrodynamic friction coefficient large enough for experimental detection. Measurements of the diffusion coefficient of sufficiently small lipid liposomes were performed,[14] and depletion effects were detected. However, a well-pronounced discrepancy between the experimental results and the theoretical predictions was found. The change of the hydrodynamic friction coefficient of the liposomes due to depletion was unexpectedly small. In addition, relatively thin depletion layers were calculated from electrophoretic experiments with small liposomes.[15−17]

When discussing polymer depletion effects at interfaces, it has to be realized that it takes a certain time for the polymer to form a depletion layer. So far this has not been taken into account in the theoretical description of polymer depletion layers. This and the above-noted experimentally found discrepancies between the static, free-energy-based theoretical description of the depletion effect and the experimental results led us to the conclusion that a dynamic effect of the particle size on the depletion layer might be present.

Although our former experiments were not designed toward the investigation of this relaxation effect, a

* Author to whom correspondence is addressed.
[†] University of Rostock.
[‡] EMBL Heidelberg.
[§] MPI for Colloid and Interface Research.
[||] University of Bristol.
[⊗] Abstract published in *Advance ACS Abstracts,* November 15, 1996.

(1) Fleer, G. J.; Scheutjens, J. M. H. M.; Cohen Stuart, M. A.; Cosgrove, T.; Vincent, B. *Polymers at Interfaces*; Chapman and Hall: London, 1993.
(2) Vincent, B.; Edwards, J.; Emmett, S.; Croot, R. *Colloids Surf.* **1988**, *31*, 267.
(3) Chauvetau, G.; Tirrel, M.; Omari, A. *J. Colloid Interface Sci.* **1984**, *100*, 41.
(4) Allain, C.; Ausserre, D.; Rondelez, F. *Phys. Rev. Lett.* **1982**, *49*, 1694.
(5) Cowell, C.; Vincent, B. *J. Colloid Interface Sci.* **1982**, *87*, 518.
(6) Li-In-On, F. K.; Vincent, B.; Waite, F. A. *J. Colloid Interface Sci.* **1987**, *116*, 305.
(7) Emmett, S.; Vincent, B. *Phase Transitions* **1990**, *21*, 197.
(8) Lambe, R.; Tadros, Th.F.; Vincent, B. *J. Colloid Interface Sci.* **1978**, *66*, 77.
(9) Prestidge, C.; Tadros, Th.F. *Colloids Surf.* **1988**, *31*, 325.
(10) Bäumler, H.; Donath, E. *Stud. Biophys.* **1987**, *120*, 113.
(11) Donath, E.; Pratsch, L.; Bäumler, H. J.; Voigt, A.; Taeger, M. *Stud. Biophys.* **1989**, *130*, 117.
(12) Bäumler, H.; Donath, E.; Pratsch, L.; Lerche, D. In Stoltz, J. F., Donner, M., Copley, A. L., Eds.; *Hemorheologie et Agregation Erythrocytaire*; Editions Medicales Internationales: Cachan, Cedex, 1991; p 24.
(13) Bäumler, H.; Donath, E.; Krabi, A.; Knippel, W.; Budde, A.; Kiesewetter, H. *Biorheology* **1996**, in press.
(14) Donath, E.; Krabi, A.; Nirschl, M.; Shilov, V. M.; Zharkikh, M. I.; Vincent, B. *Faraday Trans.* **1996**, in press.
(15) Donath, E.; Krabi, A.; Allan, G.; Vincent, B. *Langmuir* **1996**, *12*, 3425.
(16) Ermak, D. L. *J. Chem. Phys.* **1975**, *62*, 4189.
(17) Lax, E. *Taschenbuch für Chemiker und Physiker;* Bd.1, Springer Verlag: Berlin, Heidelberg, New York, 1967.

S0743-7463(96)00489-1 CCC: $12.00

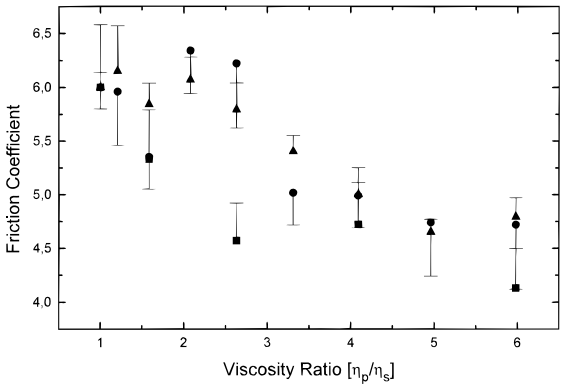

Figure 1. Friction coefficient of liposomes of different diameters in 110 kD dextran as a function of the dextran concentration expressed in viscosity ratios: triangles, 50 nm liposomes; squares, 100 nm liposomes; circles, 200 nm liposomes. η_p denotes the static viscosity of the polymer solution, while η_s is the viscosity of the solvent.

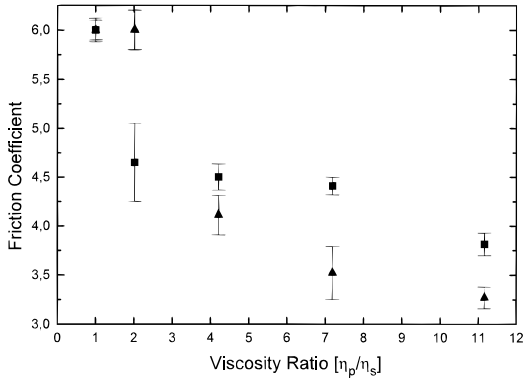

Figure 2. Friction coefficient of liposomes of different diameters in 500 kD dextran as a function of the dextran concentration: 100 nm liposomes (squares); 200 nm liposomes (triangles).

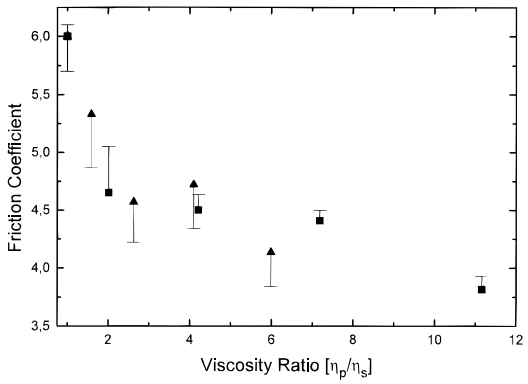

Figure 3. Friction coefficient of liposomes in 110 and 500 kD dextran as a function of the dextran concentration: triangles, 110 kD dextran; squares, 500 kD dextran. Liposome mean diameter = 100 nm.

semiempirical interpretation suggested the effect of the particle size on the depletion parameters. Obviously, the finite time necessary for the formation of the depletion zone by the polymers is a critical parameter for the formation of the depletion layer. If, in the instance of small enough particles, their diffusive motion is too fast, then the polymer depletion layer might not be completely formed. In this paper we provide a first semiquantitative theoretical explanation of this polymer relaxation effect on the basis of consideration of the various characteristic time constants in the system. We are aware of the preliminary nature of this report but think that the consequences of this new effect will be far-reaching.

Experimental Evidence of Relaxation Effects

The experimental details of the liposome preparation, the light scattering, and electrophoretic experiments are given elsewhere.[14,15] Special attention was given to the problem of avoiding misinterpretation of light scattering data due to the presence of the polymers.[14]

We start with the presentation of light scattering data of liposomes of different size in various molecular weight dextran solutions. In Figure 1 the apparent friction coefficient of liposomes of various diameter is plotted as a function of the bulk 110 kD dextran concentration. The apparent friction coefficient is a convenient parameter to characterize the depletion effect.[14] It is calculated from the experimental diffusion coefficient, assuming spherical particles and was always normalized to the bulk viscosity, η_p, times πa, where a is the particle radius. For the calculation of the friction coefficient the polymer solution is assumed to be Newtonian;[14] thus, η_p represents the static viscosity limit. The ideal case of a constant viscosity without depletion effects corresponds, consequently, to a friction coefficient of 6. Due to the depletion effect, the friction coefficient is reduced below 6. Within the limitations of the quasi-flat hydrodynamic approach, the friction coefficient can reach a theoretical minimum of 4.[14]

Even given the relatively large error of the experimentally determined diffusion coefficients, it is obvious that the particles with a diameter of 50 nm had a significantly larger friction coefficient than the 100 nm liposomes in the range of smaller bulk polymer concentrations. This was contradictory to our original expectations. For a depletion layer of constant thickness one would expect a reduction in the friction coefficient of the particles with decreasing particle size due to the reduced viscosity in the depletion zone; the depletion effect should scale with the ratio depletion layer thickness/particle radius. This follows from hydrodynamic considerations published recently.[14] In Figure 1, the 200 nm liposomes, on the other hand, appear to show the expected behavior. With increasing bulk polymer viscosity the friction coefficient decreased for all sizes. This is the consequence of the relatively steeper viscosity reduction in the depletion layer for higher bulk viscosities. It can also be seen in Figure 1 that at high polymer concentrations the anomalous behavior of the friction coefficient as a function of the particle radius is less pronounced.

The anomalous behavior of the friction coefficient is also seen in Figure 2 for a larger molecular weight dextran. While in Figure 1 the 200 nm liposomes in 110 kD dextran at least have a friction coefficient not smaller than the 100 nm liposomes, this tendency is reversed in the case of the 500 kD dextran. Obviously, the time of depletion layer formation, the relaxation time, had increased in the 500 kD dextran and, consequently, the diffusive motion of the 100 nm liposomes was too fast to allow for a complete formation of the depletion layer for the larger polymer molecular weight.

The normal, as well as the anomalous behavior, is also clearly seen when we compare liposomes of the same size in different molecular weight dextran solutions. The 100 nm liposomes in 500 kD dextran showed a friction coefficient which was not smaller than that in 110 kD dextran (see Figure 3). If the particle was at rest, one would expect a smaller friction coefficient in 500 kD dextran due to the larger extension of the depletion layer. This was, however, found when we made the same comparison with larger liposomes, as demonstrated in Figure 4. Obviously, the 200 nm liposomes are "slow" enough to guarantee now a more complete formation of the depletion layer in the larger molecular weight dextran.

In the highest polymer concentrations in some instances the measured friction coefficients decreased below 4. This is smaller than the theoretical limit.[14] A possible explanation for this behavior might be the neglect of the particle curvature in ref 14 where always thin depletion layers compared to the particle radius were assumed.

It has to be expected that the relaxation effect associated with depletion layer formation should also be apparent from other measurements, not only diffusion or friction coefficients, since this relaxation effect is an inherent property of the polymer–particle system. It should also have consequences for the interpretation of both electrophoretic measurements and colloid

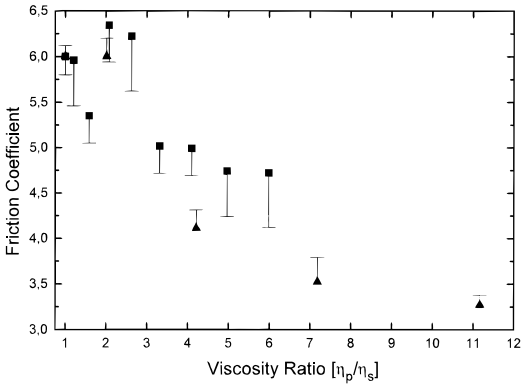

Figure 4. Friction coefficient of liposomes in 110 and 500 kD dextran as a function of the dextran concentration: squares, 110 kD dextran; triangles, 500 kD dextran. Liposome mean diameter = 200 nm.

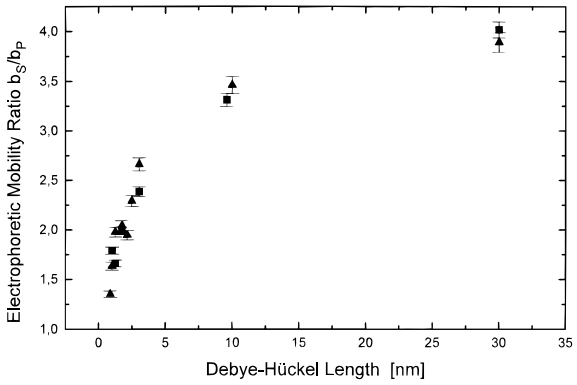

Figure 5. Electrophoretic mobility ratio of liposomes of 100 nm diameter as a function of ionic strength: triangles, 6 wt % 110 kD dextran; squares, 4 wt % 500 kD dextran.

stability data. Such systematic studies, where the particle size has been varied over the appropriate range, to our knowledge, have not been attempted yet. Finally, in Figure 5 we show electrophoretic measurements of 100 nm liposomes in 110 and 500 kD dextran. The electrophoretic mobility ratio, a convenient measure of the depletion effect, apparently is the same for two different molecular weights, which previously was difficult to explain. From electrophoretic measurements relatively small depletion layer thicknesses at liposome surfaces were also inferred, which was contradictory to measurements with human red blood cells, which have, however, a much larger size.

Semiquantitative Theoretical Analysis of the Relaxation Effect

It is clear that in order to investigate quantitatively the relaxation effect it is necessary to explore the statistical mechanics of the three-component system solvent/polymer/particle. At present such a theory is not available. Current approaches reduce the problem to the distribution of the polymer near a resting wall. Since such theories are quite complex, we present here a simpler alternative approach based on the comparison between the time of formation of the depletion layer at a resting interface, τ_{pol}, with the mean time the particle requires to diffuse over a distance equal to the depletion layer thickness, τ_{par}.

The particle diffusion time is given by the Smoluchowski equation:

$$\tau_{par} = \delta^2/2D \tag{1}$$

Here δ denotes the thickness of the depletion layer. D is the diffusion coefficient of the particle. In principle, D is a function of the depletion layer viscosity characteristics.

It is much more difficult to calculate the time of formation of the depletion layer: The existence of the depletion layer in most cases is an entropic effect. The decreased segment density in the depletion layer is a result of the necessary reduction in configurational entropy of the polymer close to the particle interface. In contrast to the possibility of considering "instantaneous" values of the free polymer energy, it is not meaningful to discuss an instantaneous value of the entropy of a polymer molecule. Entropy is, by definition, closely related to the behavior of the polymer over time. From these considerations it follows that the characteristic time of formation of the depletion layer is equal to the time necessary to "measure" the entropy of the polymer layer in a hydrodynamically sufficiently homogeneous region at the particle interface. If a sufficiently large ensemble of polymer molecules is considered, then ensemble averaging suggests that such a characteristic time is given by the decay time of the autocorrelation function of the individual polymer molecule structure, τ_{corr}. Below we used the autocorrelation function of the radius of gyration of the polymer to estimate τ_{corr}. But, if the number of polymer molecules in the hydrodynamically homogeneous region of the particle interface is too small, τ_{corr} is too short to provide a reasonable measure of the characteristic time of formation of the depletion layer. In the limiting case of a single polymer molecule it is obvious that the molecule has to "diffuse" over a sufficiently large number of configurations in the available configurational space to provide a meaningful measure of the characteristic entropic time, τ_{ent}. From these considerations it follows that the characteristic time of formation of the depletion layer, τ_{pol}, is a function of both the individual structural autocorrelation time of a single polymer and the number of molecules in the depletion layer. In a linear approximation one may write

$$\tau_{pol} = \tau_{ent} - (\tau_{ent} - \tau_{corr})\frac{n-1}{n + n_{crit} - 1} \tag{2}$$

Here n denotes the number of molecules in the hydrodynamically sufficiently homogeneous region of the depletion layer; n is a function of both the particle size and the polymer concentration. We used as a rough estimate for n the number of molecules in the depletion zone surrounding half of the particles hemisphere.

$$n = a^2/R^2 \tag{3}$$

Here a denotes the particle radius; R is the concentration dependent apparent radius of the polymer.

n_{crit} denotes the minimum number of molecules necessary to calculate τ_{pol} by means of ensemble averaging with a given precision using τ_{corr} as the characteristic time of the formation of the depletion layer. Below we used for n_{crit} a value of 30. This was justified from numerical simulations, as demonstrated below, where it is shown that a sufficiently precise estimate of τ_{ent} is given by

$$\tau_{ent} = 30\tau_{corr} \tag{4}$$

This relationship leads to values for τ_{ent} with a precision of about 3%.

In addition, it has to be ensured that the mean time for the polymer to diffuse over the distance equal to the depletion layer thickness is smaller than τ_{pol}. Otherwise, this diffusion time, τ_{diff}, determines the characteristic time of formation of the depletion layer and replaces τ_{pol}. τ_{diff} can be calculated by means of Kuhn's formula for the

polymer diffusion coefficient neglecting polymer interaction

$$D_{\mathrm{pol}} = \frac{kT}{7.4\pi\eta R_{\mathrm{g}}} \tag{5}$$

together with Smoluchowski's equation. Here k is the Boltzmann constant, T is absolute temperature, R_{g} is the radius of gyration, and η denotes the viscosity of the solvent.

Assuming again linear behavior, it follows that the depletion effect, expressed as a percentage, ϵ, is given by

$$\epsilon = 100\left(1 - \frac{\tau_{\mathrm{pol}}}{\tau_{\mathrm{pol}} + \tau_{\mathrm{par}}}\right) \tag{6}$$

A value of ϵ of 100% corresponds to the situation of a depletion layer near a stationary wall, while $\epsilon = 0$ implies absence of a depletion effect.

In order to calculate ϵ, it is necessary to find the dependence of both τ_{corr} and τ_{ent} on the number of segments in the polymer chains. This was achieved by means of a Brownian dynamics simulation.

Description of the Effected Brownian Dynamics Simulations

Methods. Brownian dynamics simulations of model polymers were effected in order to obtain estimations for the dependency of the characteristic times τ_{corr} and τ_{ent} on the polymer size. A polymer was represented by a chain of N nonpenetrable, spherical segments ("beads") with a bead radius R_{bead} of (usually) 2.27 Å. This distance is equivalent to half of the monomer−monomer distance in polyglucose, as given by the distance between the oxygen atoms in positions 1 and 4 of glucose (polymerization sites) provided by the monomer library of the program InsightII (Biosym Technologies, Inc.). The distance between the centers of consecutive beads was $2R_{\mathrm{bead}}$. The Brownian dynamics of the model polymer in an aqueous solution was simulated by using the algorithm proposed by Ermak and McCammon (1978). The simulations were performed with and without consideration of hydrodynamic interactions (HI). The position $\vec{r}$ of a bead monomer evolved according to eq 7:

$$\vec{r}_i(t+\Delta t) = \vec{r}_i(t) + \frac{\Delta t}{k_{\mathrm{B}}T}\sum_{j\neq i} D_{ij}(t)\,\vec{F}_{\mathrm{c}}(t) + \Delta\vec{r}_{\mathrm{G},i} \tag{7}$$

where the vector $\Delta\vec{r}_{\mathrm{G},i}$ represents a stochastic displacement of a monomer due to Brownian motion. Its elements were obtained from a Gaussian distribution with a mean equal to zero and the variance−covariance $\langle r_i r_j\rangle = 2D_{ij}\Delta t$. In simulations ignoring HI, D_{ij} correspond to single, scalar values, represent the diffusion coefficient of the monomer, and were calculated from the Stokes−Einstein equation, $D = k_{\mathrm{B}}T/(6\pi\eta R_{\mathrm{bead}})$, where η is the solvent viscosity ($\eta = 10^{-3}$ Pa s). In systems with considered HI, they represent 3×3 submatrices of the hydrodynamic interaction tensor denoted by Q. (The elements of Q and the algorithm for taking the square root of Q are given in the Appendix.) T is the absolute temperature (T = 298 K), Δt is the simulation time increment, and $\vec{F}_{\mathrm{c}}$ is a force satisfying the geometic constraint of the polymer, i.e., connectivities and excluded-volume interactions, and was derived from the negative gradient over the sum of all pairwise interactions with an underlaying constructed harmonic pairwise potential V_{ij}, defined as

$$V_{ij}(r) = \frac{k_{\mathrm{B}}T}{4D\delta t}(2R_{\mathrm{bead}} - r_{ij})^2 \tag{8}$$

where r_{ij} is the distance between the centers of beads i and j. For interactions of beads not consecutive in sequence, the potential was applied only if $r_{ij} < 2R_{\mathrm{bead}}$ (overlap). The time step of the simulation Δt was adjusted such that average displacements were small compared to R_{bead}. Its value was 3.38×10^{-13} s, obtained from the condition $6(2\Delta tD)^{1/2} = 0.5R_{\mathrm{bead}}$. The simulations were initiated from random, non-self-overlapping polymer chains. As characteristic measures of the structural changes in time, the radius of gyration (eq 9) and the end-to-end distance l were monitored with

$$R_{\mathrm{g}} = \sqrt{\frac{1}{N}\sum_{n=1}^{N} {R_n}^2} \tag{9}$$

where R_{n} is the distance of the center of segment n to the center of mass (geometric center).

Brownian Dynamics Results. *(a)* $\tau_{corr} = \tau_{corr}(N)$. Relationship a was expected to obey a power law of the type $\tau_{\mathrm{corr}} = aN^b$ where a and b are constants. τ_{corr} is defined as the decay time of the autocorrelation function of $R_{\mathrm{g}}(t)$ and $l(t)$ (end-to-end distance) to the value $1/e$. From simulations not including HI, we obtained, from a linear regression analysis of the observed data, $\tau_{\mathrm{corr}}(N)$ with N = 5, 10, 15, 25, 50, 75, and 100, respectively, on a log−log scale, as demonstrated for τ_{Rg} in Figure 6 (circles):

$$\tau_{\mathrm{corr},R_{\mathrm{g}}} = 1.67N^{2.44}\ \mathrm{ps} \quad \text{and} \quad \tau_{\mathrm{corr},l} = 2.796N^{2.28}\ \mathrm{ps} \tag{10}$$

Varying the bead radius and thus the diffusion coefficient of the beads resulted in a modified preexponential factor a but did not change the exponent b itself. The variations in a were observed to be linearly dependent on R_{bead} (data not shown). To judge the effect of changing the arbitrary values of the bond and excluded-volume potential (eq 8), the simulation was repeated with a modified potential by introducing a factor 0.5 to all pairwise interactions. Virtually no changes could be observed as compared to the original simulations. The excluded-volume interaction was observed to sensitively influence the scaling behavior. By switching off all nonlocal interactions; i.e., a chain of fully interpenetrable beads (Rouse model[18]), $\tau_{\mathrm{corr},l} \propto N^{1.86}$, was obtained.

Including hydrodynamic interactions corresponding to the Zimm model in the theory[18] resulted in a considerable effect on the chain dynamics. The exponent b was diminished as opposed to the non-HI case (Figure 6, triangles). The corresponding power laws are

$$\tau_{\mathrm{corr},R_{\mathrm{g}}} = 6.846N^{1.74}\ \mathrm{ps} \quad \text{and} \quad \tau_{\mathrm{corr},l} = 9.603N^{1.66}\ \mathrm{ps} \tag{11}$$

Due to the time-consuming computation of the hydrodynamic interactions, the simulations were limited to shorter polymer chains (N = 5, 10, 15, 20, and 25).

(b) $\tau_{ent} = \tau_{ent}(N)$. The correlation time τ_{ent} should provide an estimation for the time interval necessary for a polymer molecule to explore the configurational space, i.e., time periods in which restrictions in the accessibility of the total configurational space are generally "experienced" by the molecule and would result in a reduced entropy.

(18) Doi, M.; Edwards, S. F. *The Theory of Polymer Dynamics;* Clarendon Press: Oxford, U.K., 1986.

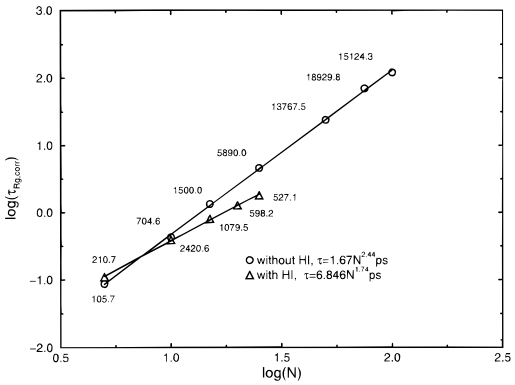

Figure 6. log−log plot of the autocorrelation time τ_{corr} *versus* the number of monomers N. The correlation coefficient r is given in the graph. Indicated at the points are the total simulation times of the runs used to derive τ_{corr}.

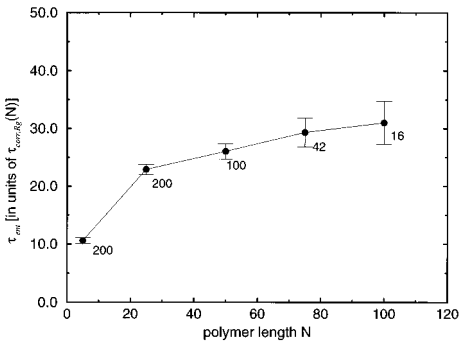

Figure 7. Dependency of the characteristic correlation time τ_{ent} (for definition see text) on the polymer size. Indicated at the points are the numbers of data used for obtaining the averaged τ_{ent} and the corresponding standard errors.

τ_{ent} was estimated from the decay of the relative standard error s_{rel} of the determination of the mean Rg in a simulation run as given by eq 12:

$$s_{rel} = \frac{\sigma_{R_g}}{\sqrt{i}\langle R_g \rangle_i} \times 100\% \qquad \text{with } i > 2 \qquad (12)$$

where σ_{R_g} is the standard deviation of the radius of gyration measured at intervals of $\tau_{corr,N}$ corresponding to the particular polymer length N obtained above and i is the number of measurements. s_{rel} was required to be smaller than 3% as a compromise between accuracy ($i > 2$) and consumed CPU time. The corresponding, repeatedly elapsed simulation times were used to estimate τ_{ent}. Figure 7 shows the dependency of the correlation time τ_{ent} defined in this way on the polymer size. Apart from the obvious scatter, the graph shows that, with increasing polymer length, τ_{ent} expressed in units of $\tau_{corr,N}$ seems to approach a constant value. In our semianalytic calculations outlined above, the relation $\tau_{ent} = 30\tau_{corr,N}$ was used as a rough estimate.

(c) $R_g = R_g(N)$. For freely-jointed chains,[19,20] the radius of gyration R_g is related to the number of monomers N by eq 13:

$$\frac{\langle R_g^2 \rangle}{N 4 R_{bead}^2} = \frac{1}{6}(N+2)/(N+1) \qquad (13)$$

Considering the limited influence of the term $(N + 2)/(N + 1)$ for large N we obtained for $N = 25$, 50, 75, and 100, respectively, and averaging over 5000 random trial structures each from a linear regression to the log−log data ($r = 0.999$):

$$R_g = 2.7669 N^{0.548}\ \text{Å} \qquad (14)$$

For $N = 1$ eq 14 yields $R_g = 2.7669$ Å. This value is very close to R_{bead}. The exponent of 0.548 thus being greater than 0.5 reflects the influence of the excluded-volume effect.

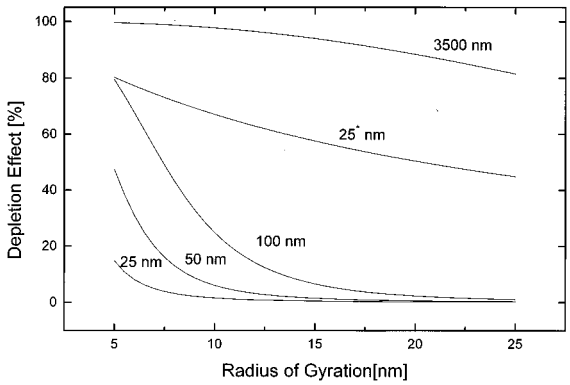

Figure 8. Theoretical depletion effect as a function of the particle and polymer size (radius of gyration) in the absence of hydrodynamic interactions. The particle radius is given at the curves. The upper 25 nm curve indicated by an asterisk corresponds to the situation where we hypothetically assumed that the polymer coverage of the particle was infinitely high (see text). The polymer concentration was such that the radius of gyration was always equal to half the mean polymer−polymer distance.

Theoretical Results for the Depletion Effect

Having now obtained the necessary time characteristics of the polymer molecules, eq 6 provides the depletion effect as a function of either the number of monomers or the radius of gyration and the particle radius. In the previous section we derived the polymer dynamics, with and without hydrodynamic interactions, for a free polymer that has no interaction with other polymer molecules nor with the particle surface. In Figure 8 the depletion effect, neglecting hydrodynamic interaction, is plotted as a function of the particle size and the polymer radius of gyration. The polymer concentration was kept constant, such that the mean distance between the center of masses of the polymers was equal to twice the radius of gyration. It can be seen that in this concentration range the extent of depletion depends sharply on the particle radius, as well as on the polymer radius of gyration. With increasing particle radius, as well as with decreasing polymer size, the depletion effect increased strongly. It can be seen that for larger particles almost no dynamic reduction of the depletion effect is visible, while for very small particles the relaxation effect for larger polymers was so strong that almost no depletion could be found. It is also worth noting that a significant part of this relaxation effect, the reduction in the depletion effect, is caused by the limitation in applying ensemble averaging, due to the reduced number of polymers present in the depletion layer. This is demonstrated by the (upper) 25 nm particle radius curve, where it is assumed that only t_{corr} determines the relaxation effect; e.g., a hypothetical large number of polymers was assumed to be present in the depletion layer.

Neglecting the polymer−polymer interaction and intramolecular hydrodynamic interaction, we can also plot the extent of depletion as a function of the polymer

(19) Flory, P. *Statistical Mechanics of Chain Molecules;* John Wiley & Sons: New York, 1969.
(20) Allison, S. A.; McCammon, J. A. *Biopolymers* **1984**, *23*, 167.

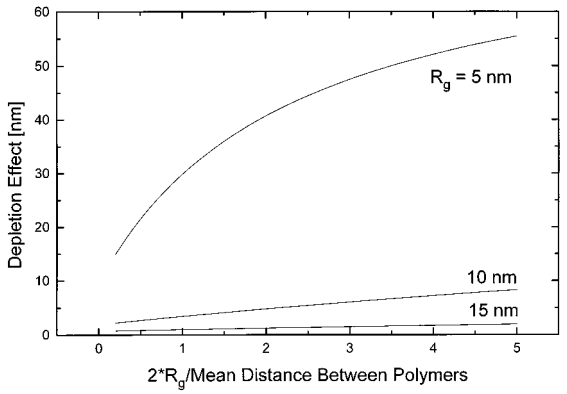

Figure 9. Theoretical depletion effect as a function of the polymer concentration for three different radii of gyration without hydrodynamic interaction. Polymer concentration is given as the ratio between the radius of gyration and half of the mean polymer−polymer distance. The particle size was 50 nm.

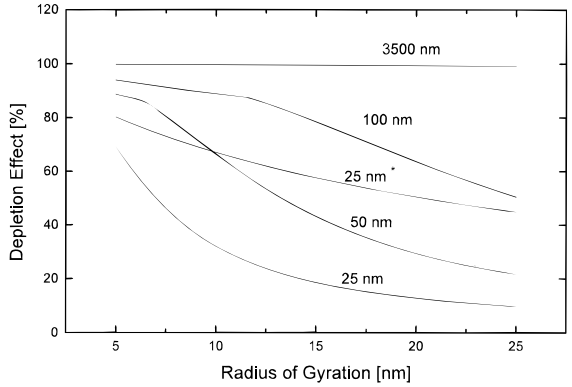

Figure 10. Theoretical depletion effect as a function of the particle and polymer size (radius of gyration) in the presence of hydrodynamic interactions. The particle radius is given at the curves. The upper 25 nm curve indicated by an asterisk corresponds to the situation where we hypothetically assumed that the polymer coverage of the particle was infinitely high (see text). The polymer concentration was such that the radius of gyration was always equal to half the mean polymer−polymer distance.

concentration, expressed in terms of the mean distance between the molecules, as is done in Figure 9. Here the abscissa value (a) denotes the ratio radius of gyration at infinite dilution/mean distance between polymers.

It can be clearly seen that increasing the polymer concentration leads to an increase of the depletion effect. The explanation is that now the larger number of polymer molecules present in the depletion zone favors the ensemble averaging and hence reduces the characteristic time constant for the formation of the depletion layer. Although a quantitative comparison with the experimental data is not directly possible, given the approximative nature of some of the assumptions used in deriving the theoretical equations, the general tendency and the order of magnitude of the effect can be discussed. The reduction of the depletion effect for larger polymers and smaller particle sizes, as shown in Figure 8, was unexpectedly large. This suggests that the theoretically calculated correlation time for the radius of gyration was too large. This was one of the reasons for incorporating the rather technically difficult problem of hydrodynamic interaction in the simulation. The consequences for the depletion effect are demonstrated in Figures 10 and 11. Due to the smaller polymer correlation time, the observed dynamical reduction of the depletion effect is significantly smaller than in the non-HI case, but for the range of polymer

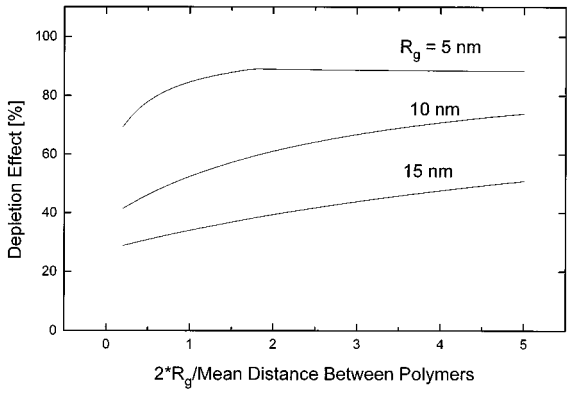

Figure 11. Theoretical depletion effect as a function of the polymer concentration for three different radii of gyration with hydrodynamic interaction. Polymer concentration is given as the ratio between the radius of gyration and half of the mean polymer−polymer distance. The particle size was 50 nm.

weights assumed, it appears to be still of the same order of magnitude.

It is worthwhile to note that the experiments fully covered the expected range of the relaxation-induced decrease of the depletion effect. For example, the 50 nm diameter liposomes in dextran 500 000 have a coverage of 1−3 dextran molecules per hydrodynamically homogeneous region. τ_{ent} determines the sampling time. However, in dextran 100 000 and with the 200 nm diameter liposomes a coverage of 20−150 molecules per half of a hemisphere as a function of polymer concentration is observed. In this case the minimum sampling time is close to τ_{corr}, which is, in turn, much smaller than the particle diffusion time over a distance equal to the depletion layer. The opposite is true for the small liposomes, where the particle diffusion time is much smaller than the τ_{ent}. These considerations apply to the case with hydrodynamic intramolecular interaction. Without this interaction the depletion would be more pronounced.

Our feeling is that the experimental effects appeared to lie somehow between the cases with and without hydrodynamic interaction. Given the approximative nature of our assumptions, as discussed below, it seems to be at present not meaningful to aim at a quantitative fit of the experimental data. The qualitative agreement is already fine. It is furthermore remarkable that the nonlinear dependence on the polymer concentration, which is contrary to theoretical expectations based on static considerations alone but observed in the experiment, could now be theoretically predicted.

We are aware of the fact that our treatment is very approximate and should by no means be considered as a final solution to the problem of the relaxation effect caused by the finite time of the depletion layer formation. Of crucial importance should be, for example, the hydrodynamic interaction with the wall and with other polymers. The wall effect should have the consequence of an apparent reduction of the monomer diffusion coefficient, thus again increasing the polymer correlation time. An interesting consequence of the spatial anisotropy should also be the breaking down of the power laws for the polymer dynamics. Polymer−polymer interaction introduces topological constraints, probably increasing the correlation time and additional hydrodynamic interactions decreasing the correlation time. The radius of curvature of the particle should also not be neglected. We plan to incorporate these ideas in future studies.

Another interesting problem is that, in the range of the dynamical reduction of the depletion effect, the fluctua-

tions of the diffusion coefficient of the particle, due to the polymer interaction, become important. This would certainly introduce a change of the shape of the autocorrelation function in light scattering experiments. The influence of this shape change on the outcome of the algorithms for calculating the apparent size of the particle from the the slope of the light scattering autocorrelation function, as is used in many commercial devices, is not known. Maybe some scatter in our experimental curves could be explained on the basis of a reduced stability of the mathematical algorithm for calculating the particle size.

Another experimental uncertainty concerns the effect of the osmotic pressure induced by the dextran addition. The possiblity of some shrinkage of the liposomes in the dextran solutions cannot be fully excluded. However, the highest molar concentrations of dextran reached only 0.5% of the ion concentration. For this reason only a marginal influence on the osmotic pressure of the solution is expected. Extra effects of dextran on the osmotic pressure due the water binding do not depend on the molecular weight and, consequently, cannot explain the observed molecular weight dependence of the depletion effect.

Regarding the electrokinetic experiments, it has to be realized that the hydrodynamically anisotropic region near the particle surface causes additional problems in the interpretation of the electrophoretic mobility of small particles. An appropriate theory describing the electrophoretic mobility for this case is not yet available. The reason is that convective contributions to the double layer polarization in the case of a significant surface curvature have to be reconsidered.

The approximative approach used here requires assumptions concerning dynamic coefficients such as the diffusion coefficients or the hydrodynamic properties near the particle surface. It is *a priori* clear that a rigorous treatment would not use these assumptions, since the equilibrium depletion layer properties, such as the mean thickness or the mean segment density distribution, should not depend on dynamic coefficients. This seeming discrepancy is explained by means of eq 8 where it is obvious that it is not the dynamic coefficient itself, but rather their ratios, which are of importance. In a rigorous treatment these ratios would depend only on the sizes and shapes of the three diffusing species.

A solution of the problem in terms of an analytical treatment seems to be at present rather difficult. Considering the electrokinetic problem, even nonequilibrium statistical mechanics in the anisotropic region near the particle interface should be combined with nonlocal hydrodynamics.

Nevertheless, we hope that the above semiquantitative treatment is not a bad approximation to the problem and believe that it might be a starting point for further experimental, as well as theoretical, studies of the polymer depletion layer relaxation effect. Clearly, systematic experimental studies are also required. There are enough open questions to give rise to further studies in this field. For example, it is of basic interest to know how the depletion layer relaxation effect on "hairy" surfaces would depend on the dynamics of the hairy surface structure.

Appendix

In this work, the hydrodynamic interactions between the subunits (beads) were approximated by the modified Rotner−Prager diffusion tensor,[22] a $3N \times 3N$ symmetric and positive definite matrix denoted by Q with 3×3 submatrices D_{ij} as elements.

The self-terms are given by

$$D_{ii} = \frac{k_B T}{6\pi\eta R_{bead}}\mathbf{I} \tag{15}$$

where η is the solvent viscosity and $\mathbf{I}$ is the 3×3 identity matrix. For identical, nonoverlapping beads and $i \neq j$, D_{ij} is calculated from

$$D_{ij} = \frac{k_B T}{8\pi\eta r_{ij}}\left[\left(I + \frac{\vec{r}_{ij}\vec{r}_{ij}}{r_{ij}^2}\right) + \frac{2R_{bead}^2}{r_{ij}^2}\left(\frac{1}{3}I - \frac{\vec{r}_{ij}\vec{r}_{ij}}{r_{ij}^2}\right)\right] \tag{16}$$

where $\vec{r}_{ij} = \vec{r}_i - \vec{r}_j$ and $r_j = |\vec{r}|$ ($r_{ij} \leq 2R_{bead}$). D_{ij} is obtained from

$$D_{ij} = \frac{k_B T}{6\pi\eta R_{bead}}\left[\left(1 - \frac{9}{32}\frac{r_{ij}}{R_{bead}}\right)I + \frac{3}{32}\frac{\vec{r}_{ij}\vec{r}_{ij}}{R_{bead} r_{ij}}\right] \tag{17}$$

Square Root of the Hydrodynamic Interaction Tensor

The stochastic displacement vector $\vec{r}_{G,i}$ in eq 7 is obtained from

$$\vec{r}_{G,i} = (\sqrt{Q}X)_i \tag{18}$$

where X is a $3N \times 1$ column vector containing random Gaussian numbers with zero mean and $2\Delta t$ variance as elements. The index $(...)_i$ denotes the elements of the resulting $3N \times 1$ vector corresponding to bead i. It is, therefore, necessary to calculate the square root of the configuration-dependent hydrodynamic interaction tensor Q. We applied an iterative, quadratically converging algorithm to derive the square root of this symmetric and positive-definite $3N \times 3N$ matrix. The symmetric and positive-definite matrix S satisfying $Q = S^2$ is iteratively obtained from

$$S_{k+1} = \frac{1}{2}(S_k + QS_k^{-1}) \tag{19}$$

with $S_0 = k_B T/(6\pi\eta R_{bead})\mathbf{I}$. In a way similar to that of Fixman,[21] the convergence was judged from the changes in S upon each iterative step. If the norm of the difference matrix $A = S_k - S_{k-1}$ was less than 0.01 times the norm of S, the iteration was exited. The norm of a matrix was defined as the root-mean-square value of all elements contained in A and S, respectively. Generally, the required precision was achieved within 2−3 iterations.

LA9604893

(21) Fixman, M. *Macromolecules* **1981**, *14*, 1710.
(22) Rotner, J.; Prager, S. *J. Chem. Phys.* **1969**, *50*, 4831.